

# GRAIN SIZE DISTRIBUTION AND GEOCHEMICAL COMPOSITION OF BADAGRY BEACH SEDIMENTS (SOUTHWEST NIGERIA): IMPLICATIONS FOR WEATHERING INTENSITY AND PROVENANCE

**\*Kazeem A. Apanpa, Adegboyega J. Adebayo and Olusegun A. Phillips**

*Department of Geology, The Polytechnic, Ibadan, Nigeria.*

*\*Author for Correspondence: [apanpa.kazeem@polyibadan.edu.ng](mailto:apanpa.kazeem@polyibadan.edu.ng)*

## ABSTRACT

Surface sediment samples collected from the foreshore of the Badagry Beach were studied for their grain size and geochemical composition in order to unveil the intensity of weathering and provenance. Wet sieving method was adopted and the sand sizes were determined from the sediment as residues for subsequent mechanical sieve analysis. Whole rock analysis using lithium tetraborate fusion was used in digestion of the pulverized beach samples. Inductively Coupled Plasma-Emission Spectrometer (ICP-ES) was used in the quantification of elements' concentrations. Particle size analysis revealed that the emplaced sediments are dominated by traction population under high energy hydrodynamic regime. Sediments are coarse grained with unimodal distribution, fine skewed, well to moderately sorted. Silica content in the sediments of Badagry Beach increases with a decrease in the concentration of soluble elemental oxides such as  $\text{Al}_2\text{O}_3$ ,  $\text{FeO}_2$ ,  $\text{CaO}$  and  $\text{MgO}$  showing linear negative trends whereas,  $\text{K}_2\text{O}$ , and  $\text{Na}_2\text{O}$  showed linear positive correlation. The CIA values for the sand-grade beach are generally  $< 50\%$ , implying sediments were generated from a source area not affected by significant chemical decomposition of minerals. Ternary plot of  $\text{Al}_2\text{O}_3$ ,  $\text{TiO}_2$  and Zr inferred sediments are enriched in heavy mineral Zr depicting compositional maturity and a reflection of crustal composition. The A-CN-K diagram revealed that the clastic sediments are richer in plagioclase than alkaline feldspar. Badagry Beach sediments have not been strongly depleted in most soluble elements such as  $\text{CaO}$ ,  $\text{Na}_2\text{O}$  and  $\text{K}_2\text{O}$  consequent upon the insignificant chemical weathering of the constituent minerals.

**Keywords:** *Weathering, Provenance, Badagry Beach, Linear negative trends, Crustal composition*

## INTRODUCTION

Grains relationship and the size distribution define 'the texture' of sediments which has assumed importance in many of its significant properties. The texture of sedimentary formation helps to infer mode and distance of transport, energy condition and depositional processes (Sharath *et al.* 2022). Sediments settle in different densities and structures, depending on the local wave action and weather, creating different textures, colors and gradients or layers of materials. The understanding of sedimentary processes, especially the environmental factors that influence weathering, transportation, deposition and subsequent modification of the sediments is crucial in determining the source and reconstructing the environment of deposition (Omotoye *et al.*, 2016). The grain size analysis is a commonly used parameter to determine the textural characteristics of sediments as all environments have their own signatures imprinted to depict different stages of denudational activities (Riyaz and Jeelani, 2015). Particle size analysis (PSA) therefore, provides important clues to the sediment provenance, transport history and depositional conditions (Folk and Ward, 1957; Friedman, 1979; Bui *et al.*, 1990).

Also, the geochemical composition of clastic sediments has been widely used to infer the provenance (Varga *et al.*, 2017), to evaluate the weathering history of the source area (Ma *et al.*, 2017), and to infer the tectonic environment (Verma and Armstrong-Altrin, 2013; 2016). The geochemistry of sedimentary formations associated with sands from beach, alluvial, and marine aeolian actions supports maturity process of the sands (Juan José *et al.*, 2007). The elemental concentrations in the various grain sizes are largely due to composition

and textural characteristics of the source rocks. The geochemical characteristics of sediments are capable of determining the distribution of trace metals in the sediments and identify any correlation. The main objectives of this study are, to determine the grain size composition and textural attributes of the sediments, evaluate the chemical elements constituting the beach sediments as well as investigate the intensity of chemical weathering, provenance, and tectonic environment.

### Study Area

Badagry Beach is located in Badagry town in the West of Lagos State, Nigeria. It is situated towards the border of the Benin Republic. The Badagry Beach area is within latitude  $6^{\circ}23'0''$  N to  $6^{\circ}24'0''$  N and longitude  $2^{\circ}48'0''$  E to  $2^{\circ}54'0''$  E (Fig. 1). The Badagry Beach is accessible by expressway, and the study location is accessible using footpath. The drainage pattern identified in the area, though not connected to the sea is dendritic as major rivers such as Ogun, Osun, Yewa and Majidun rivers are connected to the neighbouring creeks.

Geologically, Badagry lies within the coastal sands and recent alluvium of the Dahomey Basin. The geology of the Lagos area is dominated by a continuous repetition of clayey and sandy horizons. These horizons show lateral continuity in several part of the area. The lithology is made up of successions of sandy-clay, sands, clayey sands, and gravely sands, sequences. The sandy-clay layer ranges from reddish-brown to pinkish in colour. The sands units vary from very fine silty-sands to very coarse gravely sands. The sands and clay sequence have isolated intercalated bands of dark-brown to black peat. Borehole evidence indicates that the Cretaceous and Tertiary sediments underline the coastal plain sands with a general southward gentle dip, and thickening seawards.

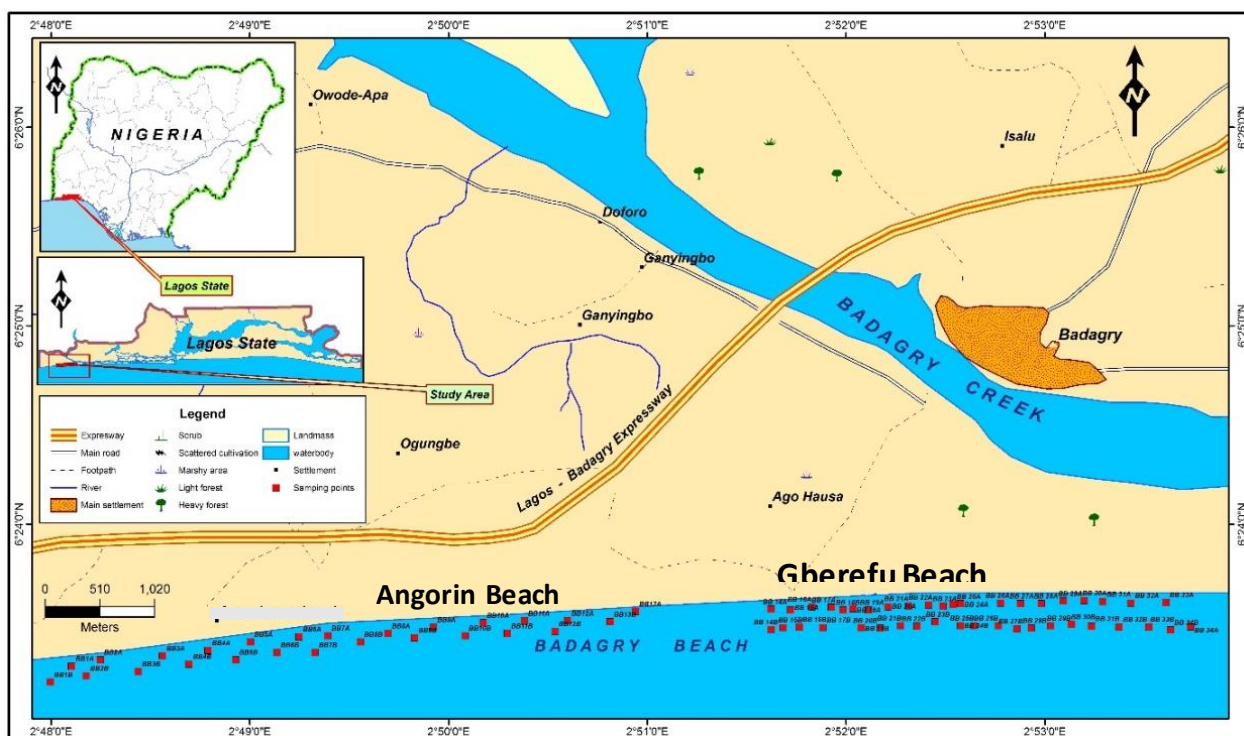


**Figure 1: Location map of Badagry Beach showing the stations sampled.**

## **MATERIALS AND METHODS**

Twenty-four surface sediment samples were collected at 200 m interval along the long-shore current direction from Angorin beach to the end of Gberefu beach fronts at Badagry. Each sample was taken from surface to the depth of about 15cm at each sampling station, using a plastic jar. Consequent upon the homogenous nature of the samples, two successive stations were added as one to bring the samples to twelve while quartering procedure was duly followed to ensure true representation of stations sampled. The Global Positioning System (GPS) was used to take coordinates at each sampled location.

The samples collected were oven dried to constant weight at temperature 45 degree Celsius before wet sieving. Two hundred and fifty grams of each sample was weighed and wet sieved through a 0.063mm sieve to separate the samples into coarse (sand and gravel retained on the sieve) and mud (clay and silt) fractions. Two hundred gram (200g) of sample was weighed from the oven dried residue gotten from the wet sieved sample (>0.063 mm fraction) and passed through a stack of nested sieve arranged in ascending order of increasing aperture sizes: 0.063mm, 0.150mm, 0.180mm, 0.212mm, 0.425mm, 0.800mm, 0.850mm, and 2.0mm, sieved for an interval of 20 minutes. Generally, the frequency for the cumulative weight percent and the corresponding phi data was subsequently used to plot and calculate the graphical statistical parameter such as Graphic mean, Inclusive graphic standard deviation, Inclusive graphic skewness and Graphic kurtosis.

The samples were analyzed for major and trace elements geochemistry. Whole Rock Analysis using Lithium Tetraborate Fusion was used in digestion of the pulverized beach sediments, as it is effective for most resistive mineral phase. The average fusion time needed was 2 hours. Standards for the ICP-AES measurements were prepared in the  $\text{Li}_2\text{BnO}_7$  flux matrix. Fusion blanks analyzed with the samples were found to contain negligible amounts of the elements of interest. (Alice *et al.*, 1992). Inductively Coupled Plasma-Emission Spectrometer (ICP-ES) was used in the quantification of elements' concentrations.

## **RESULTS AND DISCUSSION**

The results obtained from particle size analysis were used to generate various textural parameters such as Graphic Mean, Skewness and Standard Deviation by employing graphical and statistical methods. The summary of the primary and secondary data generated are presented in tables 1, 2 and 3.

### ***Textural properties***

Results from the statistical mean size (Mz) have revealed that average grain diameter ranges from 0.2 to 1.93 phi. The Badagry Beach is constituted by coarse to medium grained sand. Slight variation in grain sizes was evident along the foreshore of the beach. The overwhelming proportion of coarse grains is an indication of strong wave convergence due to the prevailing high energy conditions. Very well sorted to moderately sorted sediments predominate owing to the fact that sediments are mostly coarse sand grade.

Skewness, a measure of asymmetry of grain size population is considered a very important parameter in textural analysis because of its extreme sensitivity in subpopulation mixing. The beach sediments are mostly very fine to fine skewed except samples GB7A, GB8A and GB10A that exhibit coarse and very coarse skewed respectively. The dominance of fine skewness is a consequence of unidirectional flow of transportation agent with significant energy dissipation, whereas the coarse character implies that fine grains have been removed through strong winnowing and erosion arising from swash and backwash in the concerned stations.

Unlike skewness, kurtosis is not environment sensitive and hence does not contribute information on the depositional conditions. Kurtosis gives the degree of peakedness of a given distribution from its normal curve (Mesokurtic). The peakedness of the frequency curve is a measure of the contrast between sorting and the central part of the size distribution curve and that of the tails. Platykurtic character dominates in the beach sediment.

The aperture sizes plotted against cumulative weight % (Fig. 2) shows that the sediments have traction population, saltation population and suspended particles. The plot of aperture sizes in Phi unit against individual weight % (Fig. 3) revealed unimodal sediment which suggests a single source of sediment supply.

**Table 1: Aperture Size and the corresponding Cumulative Weight Percentage of the Beach sediments**

Sieve Size			Cummlative Weight Percent (%)											
Mm	µm	Ø	GB1A	GB2A	GB3A	GB4A	GB5A	GB6A	GB7A	GB8A	GB9A	GB10A	GB11A	GB12A
2.00	2000	-1.00	0.57	0.05	0.19	0.88	1.23	0.70	1.95	2.27	0.23	0.04	0.04	0.53
0.85	850	0.20	5.25	4.70	6.08	10.38	14.94	8.04	21.19	20.18	6.02	1.51	1.51	6.96
0.80	800	0.32	18.55	23.03	30.48	28.66	44.31	29.45	50.02	53.69	24.25	19.34	19.34	46.27
0.43	425	1.05	45.95	52.13	63.18	58.39	73.90	62.68	78.26	78.92	55.96	55.09	55.09	76.83
0.21	212	2.25	87.37	89.08	91.12	86.97	89.95	90.87	92.12	92.60	87.63	90.11	90.11	92.36
0.18	180	2.50	88.44	89.17	91.57	87.68	90.19	91.41	92.27	92.83	88.13	90.78	90.78	92.76
0.15	150	2.75	89.00	90.20	95.08	88.22	90.30	91.80	92.40	93.23	88.32	91.28	91.28	93.07
0.63	63	4.00	89.23	91.03	95.46	88.59	90.86	91.82	92.55	93.52	88.47	91.82	91.82	93.46
	PAN		95.35	95.03	95.78	95.14	96.00	95.71	95.43	95.94	93.69	95.95	95.95	95.96

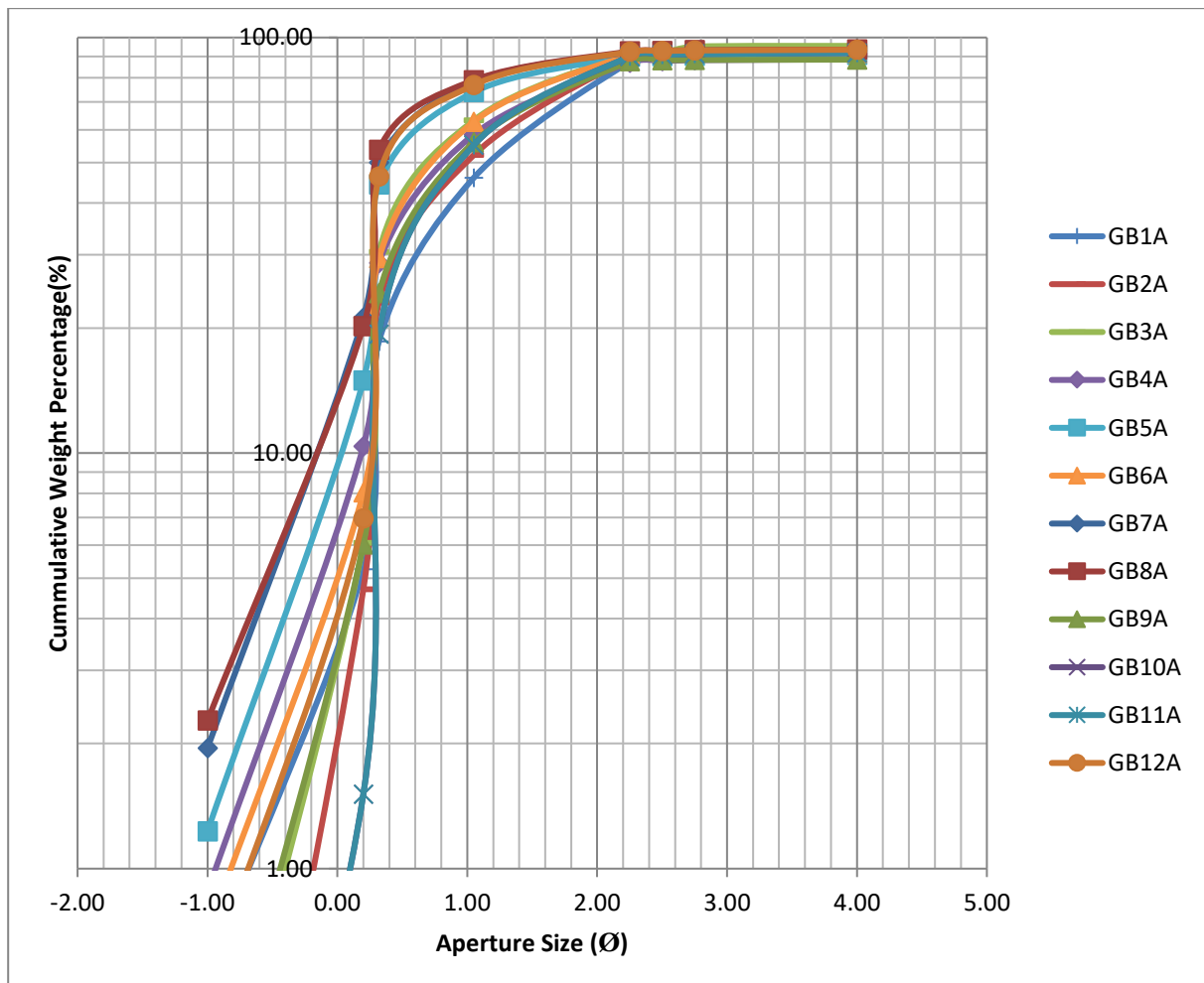


**Figure 2: The aperture sizes plotted against cumulative weight %**

**Table 2: Aperture Size and the corresponding Individual Weight Percentage of the Beach sediments**

Sieve Size			Individual Weight Percent (%)											
Mm	µm	Ø	GB1A	GB2A	GB3A	GB4A	GB5A	GB6A	GB7A	GB8A	GB9A	GB10A	GB11A	GB12A
2.00	2000	-1.00	0.57	0.05	0.19	0.88	1.23	0.70	1.95	2.27	0.23	0.04	0.04	0.53
0.85	850	0.20	4.68	4.65	5.89	9.50	13.71	7.34	19.24	17.91	5.79	1.47	1.47	6.43
0.80	800	0.32	13.30	18.33	24.40	18.28	29.37	21.41	28.83	33.51	18.23	17.83	17.83	39.31
0.43	425	1.05	27.40	29.10	32.70	29.73	29.59	33.23	28.24	25.23	31.71	35.75	35.75	30.56
0.21	212	2.25	41.42	36.95	27.94	28.58	16.05	28.19	13.86	13.68	31.67	35.02	35.02	15.53
0.18	180	2.50	1.07	0.90	0.45	0.71	0.24	0.54	0.15	0.23	0.50	0.67	0.67	0.40
0.15	150	2.75	0.56	1.03	3.51	0.54	0.11	0.39	0.13	0.40	0.19	0.50	0.50	0.31
0.63	63	4.00	0.23	0.83	0.38	0.37	0.56	0.02	0.15	0.29	0.15	0.54	0.54	0.39
	PAN		6.12	4.00	0.32	6.55	5.14	3.89	2.88	2.42	5.22	4.13	4.13	2.50
	TOTAL		95.35	95.03	95.78	95.14	96.00	95.71	95.43	95.94	93.69	95.95	95.95	95.96

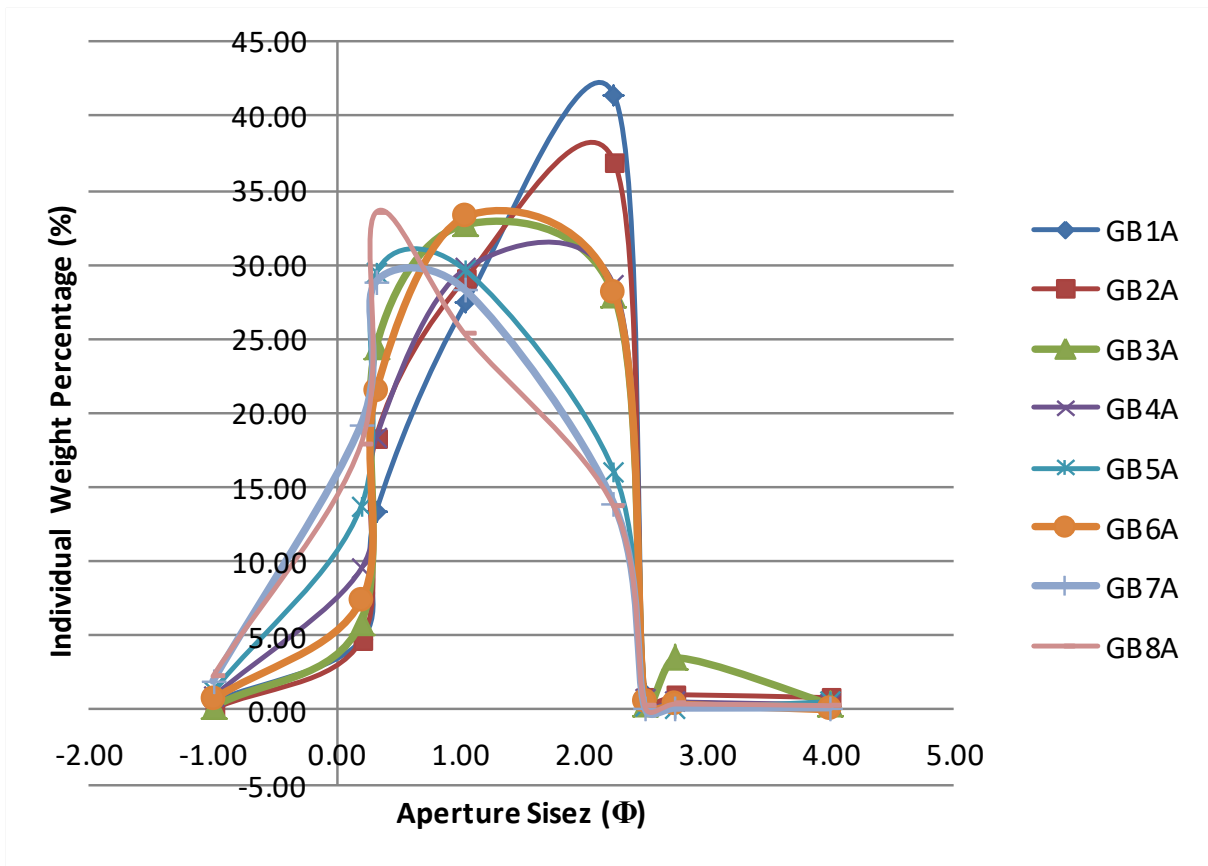


**Figure 3: Aperture Size against individual weight %**

**Table 3: Textural Properties of Sediments (Phi unit for mean, sorting, skewness and kurtosis)**

Samples	Mean	Sorting	Skewness	Kurtosis	Interpretation
GB1A	0.80	0.88	0.13	0.97	Coarse-grained sand, moderately sorted, fine skewed, and mesokurtic.
GB2A	1.93	0.98	0.40	1.42	Medium grained sand, moderately sorted, very fine skewed, leptokurtics
GB3A	1.52	-0.78	0.35	0.93	Medium grained sand, moderately well sorted, very fine skewed, mesokurtic.
GB4A	0.40	0.92	0.44	1.30	Coarse grained sand, moderately well sorted, very positive skewed, leptokurtic.
GB5A	0.36	0.31	0.25	0.00	Coarse grained sand, very well sorted, fine skewed, very platykurtic.
GB6A	0.40	0.91	0.50	1.59	Coarse grained sand, moderately sorted, very fine skewed, very leptokurtic.
GB7A	0.57	0.52	-0.27	1.34	Coarse grained sand, moderately well sorted, coarse skewed, leptokurtic.
GB8A	0.51	0.52	-5.72	0.87	Coarse grained sand, moderately well sorted, very coarse skewed platykurtic.
GB9A	0.93	0.23	8.50	-0.04	Coarse grained sand, very well sorted, very fine skewed, very platykurtic.
GB10A	0.20	0.04	-4.87	0.09	Coarse –grained sand, very well sorted, very coarse skewed, platykurtic.
GB11A	0.42	0.32	6.32	-0.08	Coarse grained sand, very well sorted, very fine skewed, very platykurtosis.
GB12A	0.67	0.26	0.71	-0.06	Coarse grained sand, very well sorted, very fine skewed, very platykurtic.

## GEOCHEMISTRY

### Major and trace element concentrations

Although the geochemical classification of sediments is not well developed, various authors have proposed few classification schemes for clastic sedimentary rocks or sediments based on their geochemical composition (Crook, 1974; Blatt *et al.*, 1980; Herron, 1988). Table 4.0 shows overall chemical composition of the sediments revealing slight variations in silica composition from 91.48 % (sample GB1A) to 93.84 % (sample GB10A). The concentration of the oxides in the sediments of Badagry Beach shows the following trend: SiO<sub>2</sub> ranges



from 91.48-93.91%,  $\text{Al}_2\text{O}_3$  1.47-1.64%,  $\text{Fe}_2\text{O}_3$  1.06-1.32%,  $\text{TiO}_2$  0.03-0.05,  $\text{MgO}$  0.09-0.2%,  $\text{CaO}$  1.08-1.15%,  $\text{Na}_2\text{O}$  0.51 - 0.56 %, and  $\text{K}_2\text{O}$  0.35-0.39%.

Sediments from Badagry beach contain  $\text{SiO}_2$  as the most dominant oxide in the sediments, confirming the sandy nature of the sediments (Figures 4 and 5).

**Table 4: Major Oxides and Trace element concentrations in weight % for the beach sands**

Samples	$\text{SiO}_2$	$\text{Al}_2\text{O}_3$	$\text{Fe}_2\text{O}_3$	$\text{MgO}$	$\text{CaO}$	$\text{Na}_2\text{O}$	$\text{K}_2\text{O}$	$\text{TiO}_2$	$\text{P}_2\text{O}_5$	$\text{MnO}$	$\text{Cr}_2\text{O}_3$	Ba	Ni	Sr	Zr	Y	Nb	SC
GB1A	91.48	1.58	1.12	0.1	1.13	0.52	0.36	0.04	0.03	0.01	<0.002	130	<20	78	36	<3	<5	4
GB2A	92.63	1.64	1.14	0.2	1.15	0.54	0.37	0.05	0.04	0.01	0.003	132	<20	77	34	<3	<5	3
GB3A	93.62	1.63	1.06	0.14	1.12	0.51	0.38	0.04	0.05	0.02	0.003	130	<20	79	35	<3	<5	4
GB4A	93.82	1.49	1.07	0.12	1.09	0.55	0.37	0.04	0.03	0.01	<0.002	128	<20	76	36	<3	<5	3
GB5A	93.58	1.5	1.09	0.1	1.1	0.53	0.36	0.03	0.02	0.01	0.002	126	<20	78	35	<3	<5	4
GB6A	93.91	1.48	1.12	0.09	1.11	0.54	0.35	0.04	0.03	0.02	<0.002	130	<20	77	36	<3	<5	4
GB7A	92.63	1.49	1.13	0.12	1.08	0.56	0.36	0.03	0.03	0.01	0.002	132	<20	76	34	<3	<5	3
GB8A	93.54	1.47	1.23	0.13	1.11	0.54	0.38	0.05	0.03	0.03	<0.002	130	<20	78	35	<3	<5	4
GB9A	93.79	1.5	1.15	0.11	1.1	0.55	0.36	0.03	0.02	0.01	0.002	132	<20	77	36	<3	<5	4
GB10A	93.84	1.5	1.11	0.1	1.11	0.53	0.38	0.05	0.03	0.01	<0.002	129	<20	78	36	<3	<5	4
GB11A	92.92	1.62	1.32	0.12	1.13	0.54	0.39	0.04	0.04	0.01	<0.002	130	<20	78	36	<3	<5	2
GB12A	93.56	1.52	1.1	0.11	1.14	0.53	0.37	0.05	0.06	0.02	0.003	131	<20	76	35	<3	<5	1

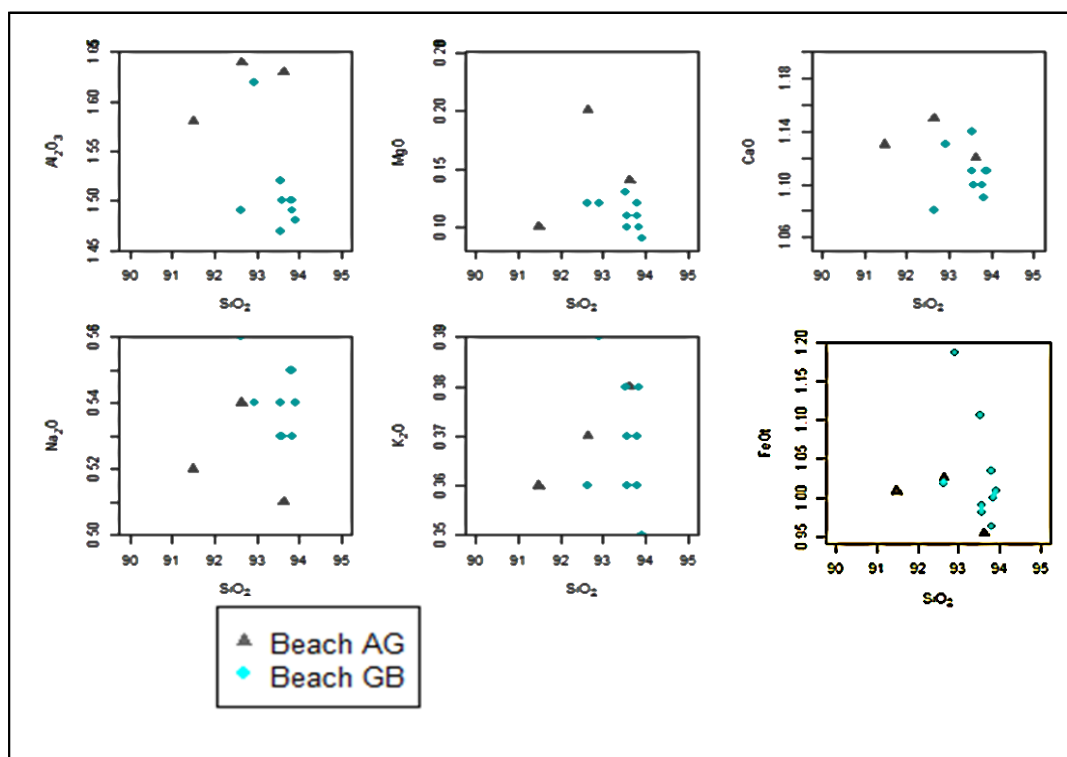


**Figure 4: Harker's Diagram for  $\text{SiO}_2$  against Major Elements**

# Research Article

Silica content in the sediments of Badagry Beach increases with a decrease in the concentration of soluble elemental oxides such as  $\text{Al}_2\text{O}_3$ ,  $\text{FeO}_2$ ,  $\text{CaO}$  and  $\text{MgO}$  indicating linear negative trends. Whereas,  $\text{K}_2\text{O}$ , and  $\text{Na}_2\text{O}$  show linear positive correlation with  $\text{SiO}_2$  (Figure 4) as the silica contents in the sediments increase with increase in the concentration of the major oxide. However, these major oxides exhibit no particular trends with aluminum (Figure 6) due to their chemical mobility potential. The silica plot against the trace elements such as Y, Zr and Sr, and ratios of  $\text{K}_2\text{O}/\text{Na}_2\text{O}$  depict no particular correlation, whereas Ba and Mg show negative linear correlation with silica (Figure 4). The aluminum plot against the trace oxides shows no linear correlation (Figure 7).

## Weathering Intensity

Chemical Index of Alteration (CIA) is a measure of weathering intensity in the source region (Nesbitt and Young, 1982). According to the A-CN-K diagram (Figure 8), un-weathered igneous rocks have CIA values near 50, whereas intensively weathered clay materials like kaolinite, gibbsite, and chlorite have values up to 100. The CIA values for the Badagry beach sands are generally  $< 50\%$ , this indicates that these sediments were generated from a source area not affected by significant chemical decomposition of minerals.

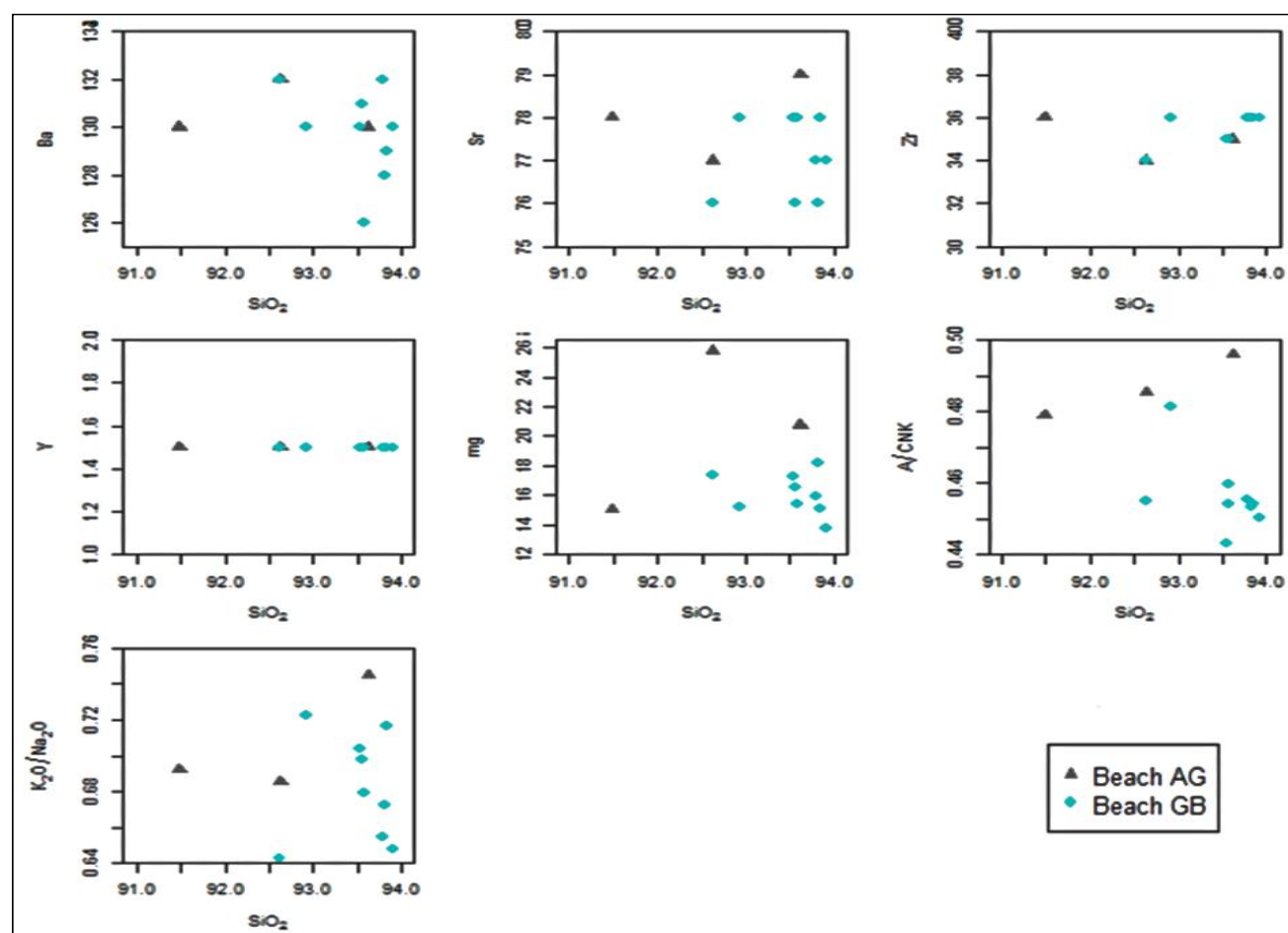


Figure 5: Harker's Diagram for  $\text{SiO}_2$  against Trace Elements



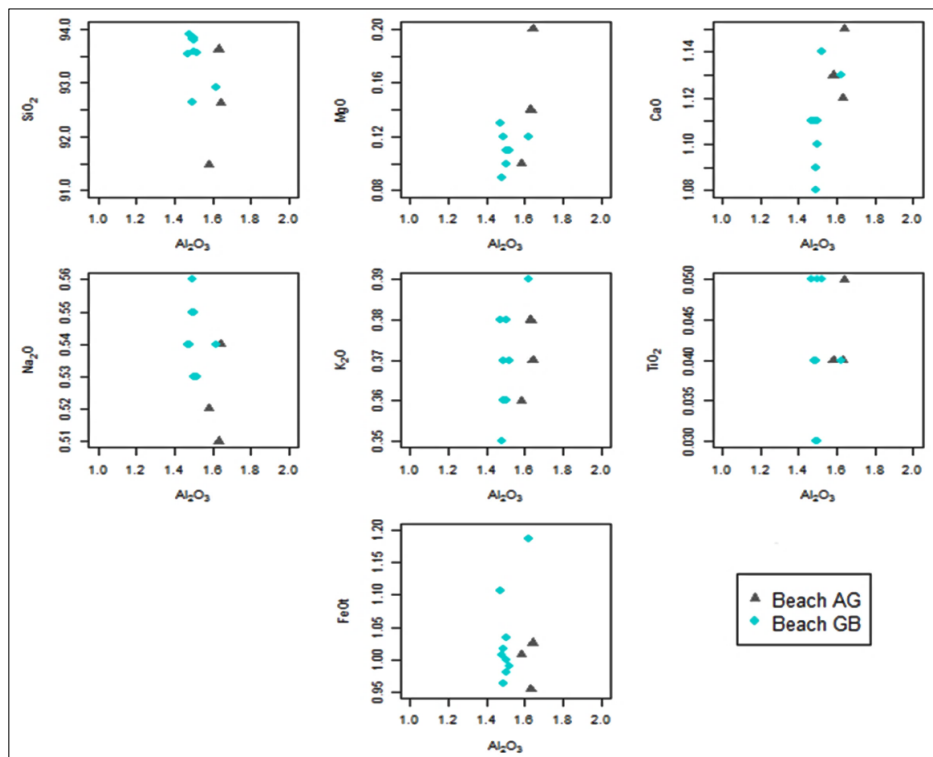


Figure 6: Harker's Diagram for  $\text{Al}_2\text{O}_3$  against Trace Elements

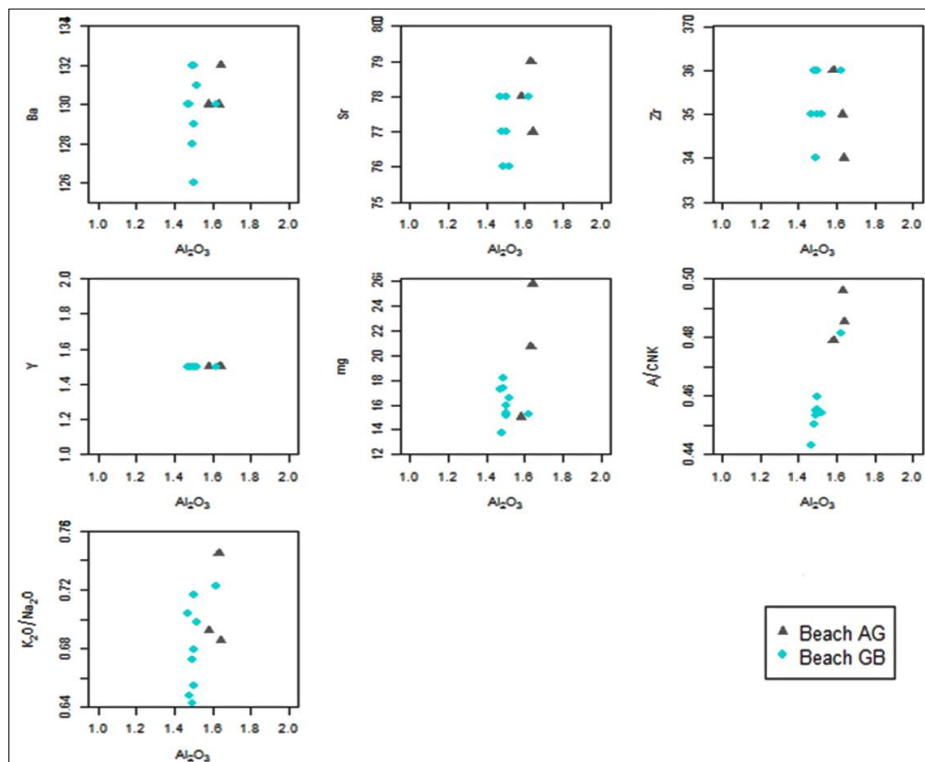
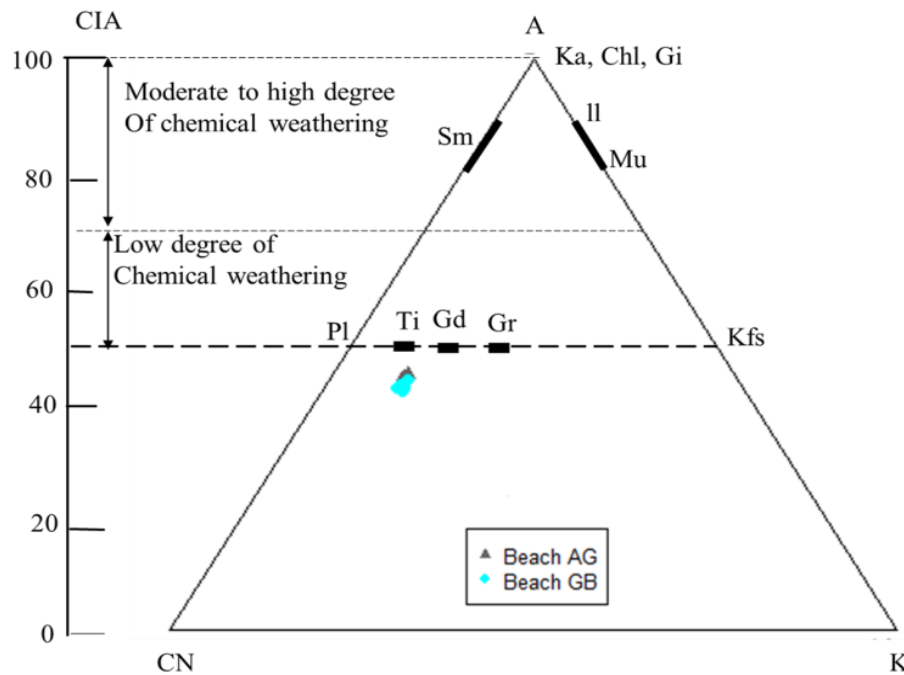
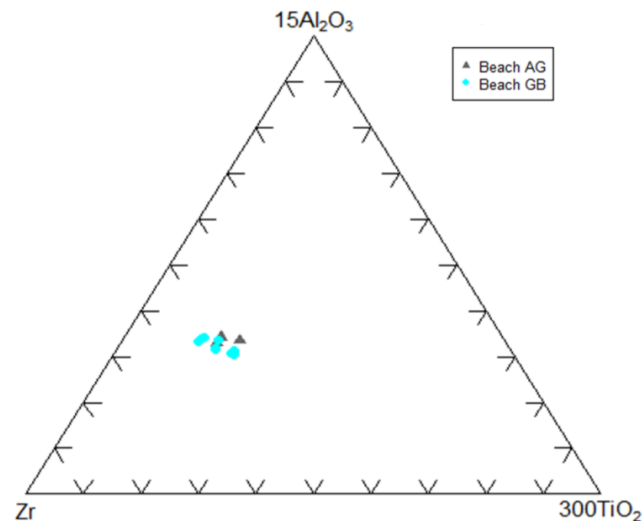


Figure 7: Harker's Diagram for  $\text{Al}_2\text{O}_3$  against Trace Elements



**Figure 8:** A-CN-K ( $\text{Al}_2\text{O}_3\text{-CaO+Na}_2\text{O-K}_2\text{O}$ ) ternary diagram with associated chemical index of alteration (CIA) after Nesbitt and Young (1982). Squares and bars symbolize average composition of tonalite (Ti), granodiorite (Gd), granite (Gr), kaolinite (Ka), chlorite (Chl), smectite (Sm), illite (Il), muscovite (Mu), plagioclase (Pl) and k-feldspar (Kfs).

Ternary plots based on  $\text{Al}_2\text{O}_3$ ,  $\text{TiO}_2$  and Zr may illustrate the presence of sorting-related fractionations recognizable by simple mixing trends on a ternary  $\text{Al}_2\text{O}_3\text{-TiO}_2\text{-Zr}$  diagram (Garcia *et al.* 1994). The plot interpreted the influence of sorting processes and provides information on the zircon concentration in sediment with a limited range of  $\text{Al}_2\text{O}_3\text{-Zr}$  (Fig. 9), indicating the sediments to be enriched in heavy mineral Zr depicting compositional maturity and a reflection of crustal composition.



**Figure 9:** Garcia's ternary plot of  $15*\text{Al}_2\text{O}_3\text{-Zr-300*TiO}_2$  showing degree of sorting in the studied sediments.

### Provenance

The ratios of  $\text{Al}_2\text{O}_3 / \text{TiO}_2$  have proven to be effective in source discrimination of clastic sediments due to the resistance of these oxides to weathering, transportation and diagenesis processes (Abu and Sunkari, 2020), and have been used to a larger extent by many workers in sediment source characterization (Garcia et al., 1994; Girty et al., 1996 and Armstrong-Altrin *et al.*, 2012). The ratios  $\text{Al}_2\text{O}_3 / \text{TiO}_2$ , and  $\text{TiO}_2 / \text{Zr}$  are good indicators of provenance (Hiscott 1984, McLennan et al. 1993, Cullers 1994, Hayashi *et al.* 1997). Mafic source rocks have  $\text{Al}_2\text{O}_3 / \text{TiO}_2$  ratios. The  $(\text{CaO} + \text{MgO})\text{-SiO}_2/10\text{-(Na}_2\text{O}+\text{K}_2\text{O})$  (Fig. 10) ternary plot shows the high presence of Silica in all minerals. The binary plot of  $\text{SiO}_2$  against  $\text{K}_2\text{O}/\text{Na}_2\text{O}$  (Fig. 11) indicates that the sedimentation is associated with active continental settings. Meanwhile, the discrimination plot of  $\text{K}_2\text{O}$  against  $\text{Na}_2\text{O}$  indicates that the sediments are classified as Quartz-intermediate (Fig. 12). The binary plot of  $\log (\text{Fe}_2\text{O}_3/\text{K}_2\text{O})$  versus  $\log (\text{SiO}_2/\text{Al}_2\text{O}_3)$  depicts Quartz arenite which reflects the composition of quartz dominating beach (Fig. 13). The high value points to compositionally matured sediments (Rashid *et al.*, 2015; Anani *et al.*, 2017).

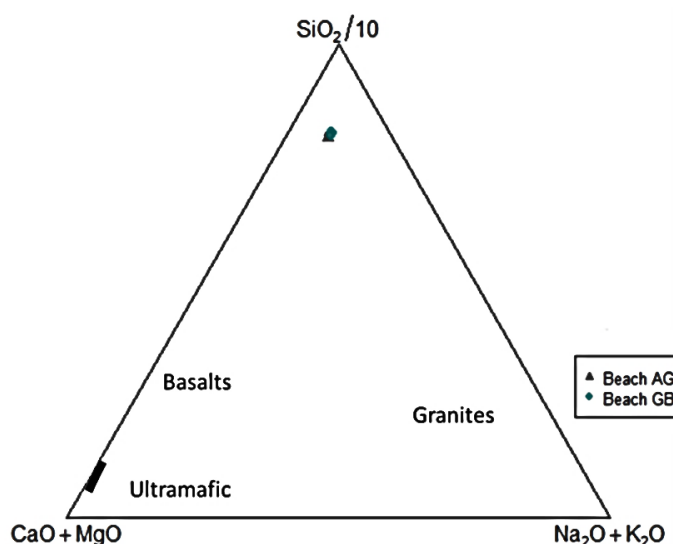


**Figure 10:**  $(\text{CaO}+\text{MgO})\text{-SiO}_2\text{-(Na}_2\text{O}+\text{K}_2\text{O})$  diagram showing comparison between major-element compositions of the analyzed samples and those of ultramafic, basalts and granites (Taylor & McLennan 1985).

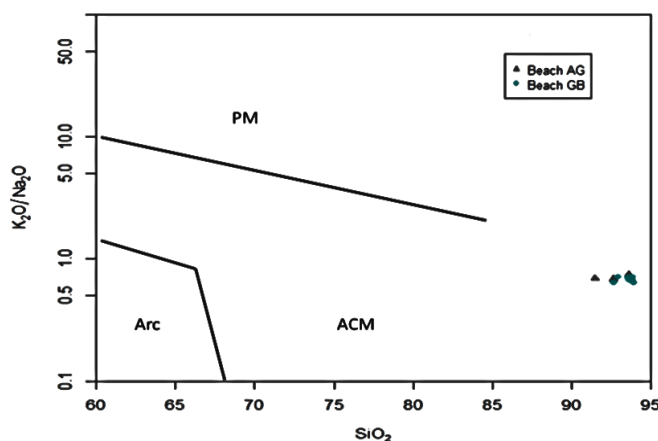


**Figure 11:** Binary plot for the samples showing tectonic setting (Roser 1986). PM- Passive continental settings, ACM- Active continental settings, Arc- Island Arc

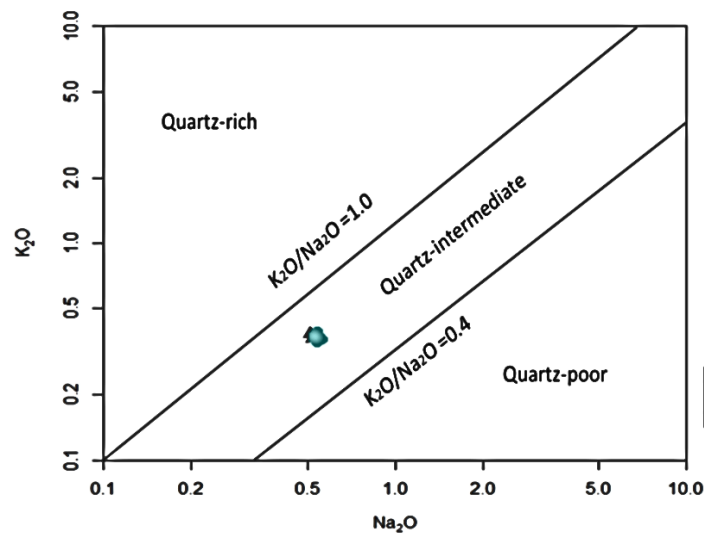


Figure 12: Plot of  $\text{Na}_2\text{O}$  versus  $\text{K}_2\text{O}$  showing quartz enrichment

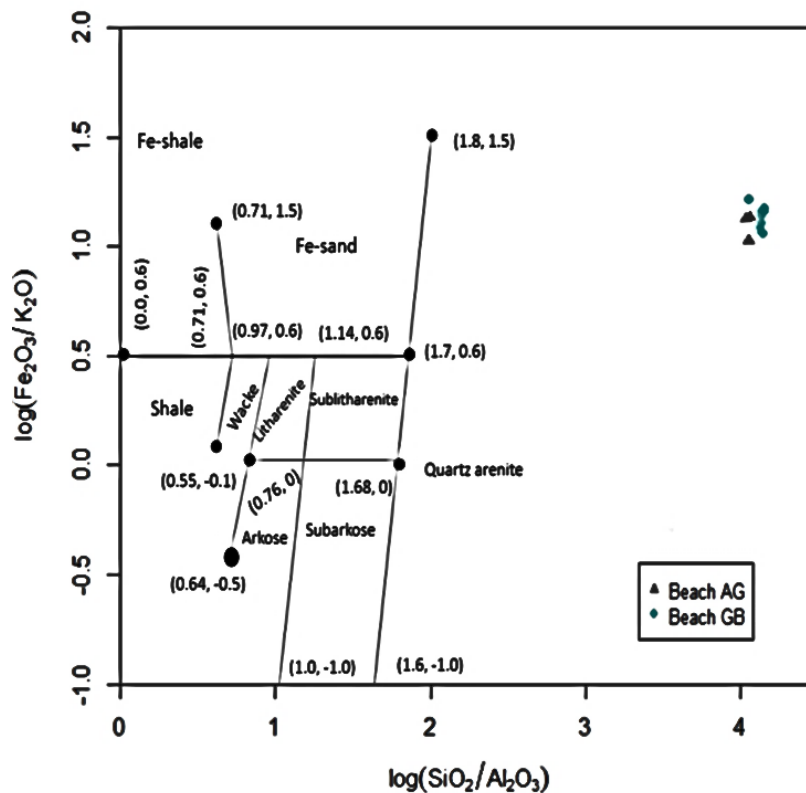


Figure 13.: The classification of Terrigenous sandstones and Shales (After Herron, 1988).

## CONCLUSIONS

The statistical mean values showed the prevalence of coarse sands. Sediments are moderately sorted, very fine skewed, and most are very platykurtic. Evidently the foreshore wind frequencies and the high energy hydrodynamic swash enabled the emplacement of mostly coarse grain and moderately sorted sediments. The

individual weight % plotted against the grain diameters unveiled unimodal distribution, inferring single source sediment. Also, sediments are chiefly constituted by traction population inferring from the log-linear graph of cumulative weight percent and particle diameters.

The A-CN-K diagram revealed that the clastic sediments are richer in plagioclase than alkaline feldspar. Badagry Beach sediments have not been strongly depleted in most soluble elements such as CaO, Na<sub>2</sub>O and K<sub>2</sub>O consequent upon the insignificant chemical weathering in the environment. The sediments which seemed to have been sourced from quartz-intermediate rocks are enriched in heavy mineral Zr. The intensity of mechanical disintegration of minerals and high degree of sediment sorting espoused with winnowing of fine particles of the sand grade beach produced quartz arenite.

## REFERENCES

- Abu M and Sunkari ED (2020).** Geochemistry, Grain Size Characterization and Provenance of Beach Sands along the Central Coast of Ghana. *Advanced Research in Chemical & Applied Sciences* **2**(1) 15-26
- Alice ME, Edmund AH and Donald GG (1992).** Innovative methods for inorganic sample preparation. *Argonne National Laboratory, Analytical Chemistry Laboratory, Chemical Technology Division, Argonne, Illinois*. 1 – 35.
- Anani C Y, Mahamuda A, Kwayisi D, Asiedu D K (2017).** Provenance of sandstones from the Neoproterozoic Bombouaka Group of the Volta Basin, Northeastern Ghana. *Arabian Journal of Geosciences* **10** 465.
- Armstrong-Altrin JS, Lee YI, Kasper-Zubillaga JJ, Carranza-Edwards A, Garcia D, Eby N, Balaram V, Cruz-Ortiz NL (2012).** Geochemistry of beach sands along the Western Gulf of Mexico, Mexico: implication for provenance. *Chemie der Erde/Geochemistry* **72** 345–362.
- Blatt H, Middleton GV and Murray RC (1980).** Origin of Sedimentary Rocks. 2<sup>nd</sup> Ed., Prentice-Hall, New Jersey, 634.
- Bui EN, Mazullo J, Wilding LP (1990).** Using quartz grain size and shape analysis to distinguish between Aeolian and Fluvial deposits in the Dallol Bosso of Niger (West Africa). *Earth Surface Processes and Landforms* **14** 157–166.
- Crook KAW (1974).** Lithogenesis and geotectonics: The significance of compositional variation in flyscharenites (greywackes). *Society of Economical, Paleontological and Mineralogical, Special Publications*, **19** 304–310.
- Cullers RL (1994).** The controls on the major and trace element variation of shales, siltstones, and sandstones of Pennsylvanian-Permian age from uplifted continental blocks in Colorado to platform sediment in Kansas, USA. *Geochimica Cosmochimica Acta*, **58**(22) 4955–4972.
- Folk RL and Ward WC (1957).** Brazos River Bar: A study in the significance of grain size parameters, *Journal of Sedimentary Petrology*, **27** 3-26.
- Friedman GM (1979).** Differences in size Distribution of Populations of Particles among Sand Grain of Various Origins. *Sedimentology*, **26** 3-20.
- Garcia D, Fontelles M and Moutte J (1994).** Sedimentary Fractionations between Al, Ti, and Zr and the Genesis of Strongly Peraluminous Granites. *The Journal of Geology*, **102**(4) 411 – 422.
- Girty GH, Ridge DL, Knaack C, Johnson D and Al-Riyami RK (1996).** Provenance and depositional setting of Paleozoic chert and argillite, Sierra Nevada, California. *Journal of Sediment Research* 66.
- Hayashi K, Fujisawa H, Holland H and Ohmoto, H (1997).** Geochemistry of ~1.9 Ga sedimentary rocks from northeastern Labrador. *Canada: Geochimica et Cosmochimica Acta*, **61** 4115-4137.
- Herron MM (1988).** Geochemical Classification of Terrigenous Sands and Shales from Core or Log data. *Journal of Sedimentary Petrology*, **58** 820-829.
- Hiscott RN (1984).** Ophiolitic source rocks for Taconic-Age flysch: trace elements evidence. *Geologic Society of America Bulletin*, **95** 1261-1267.

**Juan José KZ and Hugo Z (2007).** Grain Size, Mineralogical and Geochemical Studies of Coastal and Inland Dune Sands from El Vizcaíno Desert, Baja California Peninsula, Mexico. *Revista Mexicana de Ciencias Geológicas* **24** 423-438.

**Ma K, Hu S, Wang T, Zhang B, Qin S, Shi S, Wang K and Qingyu H (2017).** Sedimentary environments and mechanisms of organic matter enrichment in the Meso - Proterozoic Hongshuizhuang Formation of northern China. *Palaeogeography, Palaeoclimatology Palaeoecology*, **475** 176-187.

**McLennan SM, Hemming S, McDaniel DK. and Hanson GN (1993).** Geochemical approaches to sedimentation, provenance and tectonics. In: M.J. Johnson and A. Basu, (Eds.), Processes Controlling the Composition of Clastic Sediments. *Geological Society of American, Special Paper*, **32** 21-40.

**Nesbitt HW and Young (1982).** Early Proterozoic Climate and Plate Motions Inferred from Major Element Chemistry of Lutites. *Nature* **299** (5885) 715 – 717.

**Omotoye SJ, Fadiya SL and Adesiyun TA (2016).** Sedimentological Study and Heavy Mineral Analysis of Sediment Samples from Well-S, Niger Delta, Nigeria. *Universal Journal of Geoscience* **4**(3) 51-61.

**Rashid SA, Ganai JA, Masoodi A and Khan FA (2015).** Major and trace element geochemistry of lake sediments, India: implications for weathering and climate control. *Arabian Journal of Geosciences*, **8** 10481-10496.

**Riyaz-Ahmad M and Jeelani GH (2015).** Textural Characteristics of sediments and weathering in the Jhelum River Basin located in Kashmir valley, Western Himalaya. *Journal of Geological society of India*, **86** 445 – 458.

**Roser BP and Korsch RJ (1986).** Determination of Tectonic setting of sandstone-mudstone suites using SiO<sub>2</sub> content and K<sub>2</sub>O/Na<sub>2</sub>O ratio. *Journal of Geology*, **94** 635 -650.

**Sharath RB, Sujith MS, Babu N, Mohammed-Aslam MA and Lakkundi TK (2022).** Textural and Heavy Mineral Characteristics of Sediments from Chaliyar River and Adjoining Bepur Beach, Kerala: Implications to Sediment Dynamics and Provenance. *Journal of Geosciences Research*, **7**(1) 31-41.

**Taylor SR and McLennan SM (1985).** The Continental Crust: Its Composition and Evolution. *Blackwell Oxford*, 1-312.

**Varga A, Raucsik B and Szakmány G (2017).** Origin of natural arsenic antimony contents in the Permian to Lower-Triassic siliciclastic rocks of the western Mecsek Mountains, SW Hungary. *Carpathian Journal of Earth and Environmental Sciences*, **12** 5- 12.

**Verma SP and Armstrong-Altrin JS (2013).** New Multi-Dimensional Diagram for Tectonic Discrimination of Siliciclastic Sediments and their Application to Precambrian Basins. *Chemical Geology*, **355** 117 – 133.

**Verma SP and Armstrong-Altrin JS (2016).** Geochemical Discrimination of Siliciclastic Sediments from Active and Passive Margin Settings. *Sedimentary Geology*, **332** 1 – 12.

**Copyright:** © 2023 by the Authors, published by Centre for Info Bio Technology. This article is an open access article distributed under the terms and conditions of the Creative Commons Attribution (CC BY-NC) license [<https://creativecommons.org/licenses/by-nc/4.0/>], which permit unrestricted use, distribution, and reproduction in any medium, for non-commercial purpose, provided the original work is properly cited.